Sensors & Actuators: B. Chemical 316 (2020) 128138

Contents lists available at ScienceDirect

Sensors and Actuators B: Chemical

journal homepage: www.elsevier.com/locate/snb

Colorimetric cutoff indication of relative humidity based on selectively functionalized mesoporous silica

Erika Švara Fabjan[a,*], Peter Nadrah[a], Anja Ajdovec[a], Matija Tomšič[b], Goran Dražić[c], Matjaž Mazaj[c], Nataša Zabukovec Logar[c,d], Andrijana Sever Škapin[a]

[a] Slovenian National Building and Civil Engineering Institute, Dimičeva 12, 1000 Ljubljana, Slovenia
[b] University of Ljubljana, Faculty of Chemistry and Chemical Technology, Večna pot 113, 1000 Ljubljana, Slovenia
[c] National Institute of Chemistry, Hajdrihova 19, 1000 Ljubljana, Slovenia
[d] University of Nova Gorica, Vipavska 13, 5000 Nova Gorica, Slovenia

ARTICLE INFO

Keywords:
turn-on colorimetric probe
selective functionalization
mesoporous silica
relative humidity
capillary condensation

ABSTRACT

We present a novel – cutoff concept of colorimetric indication of relative humidity based on dye dissolution in condensed water in capillaries of selectively functionalized mesoporours host SiO_2 material. Consistently high levels of indoor air humidity induces mold and algae growth which represent a potential risks for human health and have deteriorating effect on walls as well. Simple localized humidity detection of high humidity with naked eye especially at places with low air circulation, where growth of mold usually starts first, is therefore highly desirable. The reporting dye was integrated in the non-functionalized mesoporous silica matrix with different pore diameters and selective-functionalized mesoporous silica material. After exposure to the environment of different air humidities the dye dissolved in water causing color change of adsorbent. With the use of adsorbents with different mesopore diameters high ability to tune the value of relative humidity when complete capillary condensation occurred was achieved. Materials with pore diameters of 3.0 nm, 3.5 nm and 7.0 nm exhibit gradual color change when reaching relative humidity up to 55, 79 and 88 RH % respectively. After selective methylation of the material with 7.0 nm pore diameter, non-gradual cutoff color change was achieved. Sample exhibited color change at narrow range of relative humidity (cutoff color change). Due to selective functionalized outer surface the dye dissolution occur only in condensed water in pores and therefore provide colorimetric indication only in this range. Selectively modified silica material has a great potential for a straightforward detection of high humid environment.

1. Introduction

Mesoporous silica materials are defined as porous materials with pore diameter in a range of 2 nm to 50 nm according to the International Union of Pure and Applied Chemistry (IUPAC) [1]. Due to the possibility of altering the material properties, mesoporous silica—together with other porous ceramic materials—show potential for their use in sensing [2,3]. There are many options for tailoring the silica pore structures, such as the diameter, orientation, shape, and geometry of the pore channels, as well as the possibility of incorporating the functional chemical groups onto the surface of pores by changing synthesis parameters such as pH, temperature, the type of surfactants, and organosilanes [4].

In humidity-sensing materials, mesoporous matrices most often present the support or skeleton of the sensing composites because their high surface area and interconnected pore channels (such as in the well-known representative of mesoporous silica materials, SBA-15) enable easier adsorption and transportation of water molecules through the surfaces [5,6]. In order to improve sensitivity and linearity of the humidity sensor response, different loading materials are dispersed into the skeleton of the mesoporous silica [7] (e.g., TiO_2 [7], SnO_2 [5], ZnO [8] $Fe(NO_3)_3$ [9]) and various functional organic groups are bonded to the silica surface [10,11].

The advantage of those electronic sensors is the accuracy of the measured value. On the other hand, measuring the RH with such a device only gives the value of RH of air in the vicinity of the sensor. However, the RH in different parts of living spaces vary due to temperature differences. Problematic areas are corners and exterior walls, where lack of ventilation and lower temperature increase RH locally. High RH enables the growth of mold, which is detrimental to both

* Corresponding author.
E-mail address: erika.svara-fabjan@zag.si (E. Švara Fabjan).

https://doi.org/10.1016/j.snb.2020.128138
Received 1 February 2020; Received in revised form 9 April 2020; Accepted 13 April 2020
Available online 19 April 2020

human health and also building appearance. International Energy Agency stated that the threshold RH for mold germination on materials in buildings is 80 % on a mean monthly basis. On paints, wallpaper, wood, gypsum and dust mold germination and growth is rarely observed under 85 % of RH) [12]. However, prompt information of locally high RH in problematic areas with easy-to-read indicators by naked eye warns the users, which can then take actions to lower the RH and prevent undesirable effects, such as mold growth.

Designing a colorimetric-sensitive material requires finding a chemical or physical process that combines a specific target stimulus and a visible color change [13]. One of the first proposed colorimetric humidity indicators was based on cobalt(II) chloride [14], which formed salts having 1 to 6 molecules of bound water. The anhydrous form is bright blue, while the hydrated one is pink. The $CoCl_2$ was also immobilized in the optical fibre [15] and the $CoCl_2$-polymer hybrid was produced, which retained colorimetric responsiveness to RH changes [16]. Despite the simplicity and effectiveness of the described humidity indicator, cobalt dichloride is a very toxic compound and was also classified by the European Union as a category-2 carcinogen.

Other dyes already used in the fabrication of humidity indicators are Ru-complex based dye [17], rhodamine [18], crystal violet [19–21] and methylene blue [22–24]. The use of methylene blue dye is the most often associated with dye aggregation and dye metachromacity. Zanjanchi and Sohrabnezhad [22] reported on integration of methylene blue in zeolite. The mechanism is based on the protonation-deprotonation reactions in protonated mordenite zeolite. Authors show linear response through the range of relative humidity 9-92 % RH. Horvath et al. [23] presented the study of dimerization of methylene blue (MB) on titanate nanowires. on metachromasity of the dye. The sensor shows linear response over 8-98 % RH. Fernández-Ramos et al. [24] reported on using MB membrane made of hydrophilic polymer hydroxypropyl methylcellulose. The sensor showed linear response in the 0-99.5 % RH. Mechanism suggested to be based on methachromasy related to dimerization of methylene blue.

The main objective of the present research was the development of a new advanced functional material for indication of RH using only naked eye in the desired range of RH. Mesoporous silica with tailored pore channels presents ideal material for indication of RH change at specific value of RH due to phenomenon of capillary condensation. It is assumed that with the exposure of mesoporous silica with comparable hydrophobicity to the humid environment, the phenomenon of capillary condensation will be triggered at the characteristic relative humidity value dependent on the diameter of the pores. There are many studies on the optical sensing of humidity by silica-based materials [25], e.g., the nanostructured coating of the SiO_2 based on the superhydrophilic film from nanoparticles with a size of 22 nm and 7 nm [26] and silica gel optical fiber humidity sensor [27] Similarly, Estella et al.[28] investigated how the porosity of non-defined xerogel film influences the sensitivity, reversibility, and reproducibility of the sensor. To the best of our knowledge, there are no reports yet on humidity indicators of the narrow range of relative humidities based on the capillary condensation in mesoporous silica.

Because the water molecules from the humid air condense at different relative humidity values in dependence on the pore diameters of the mesoporous material, the main idea of the work was to exploit the capillary-condensed water in the pores as the medium for dissolution of dye in the pores and thus the change of its color. Water condenses in the pores at characteristic relative humidity values, depending on the pore diameter of the mesoporous material. Because these materials exhibit narrow pore size distributions, this type of indicator would enable the indication of specific relative humidity based on the pore sizes of selected mesoporous material.

Herein, we present a study of relative humidity indication with mesoporous silica particles with pores of different diameters containing a reporting dye. The methylene blue has been selected as the model dye due to its nontoxicity in low concentration [29]. Furthermore, as a proof of principle, we show that selective functionalization of the external surface of mesoporous silica is crucial for achieving color change of the dye in the narrow range of relative humidity, coinciding with capillary condensation.

2. Experimental Section

2.1. Materials

Tetraethoxysilane (TEOS, reagent grade, 98 %), trimethoxy(methyl) silane (98 %), hexadecyl–trimethyl–ammonium bromide (CTAB, 99 %), decyl–trimethyl–ammonium bromide (DTAB, 98 %), methylene blue hydrate (MB, 97 %), ammonium hydroxide solution (p.a. reagent, ~25 % NH_3 basis), poly(ethylene glycol)–block–poly(propylene glycol)–-block–poly(ethylene glycol) (pluronic 123), and toluene (ACS reagent, 99.7 %) were purchased from Sigma–Aldrich. Ethanol (absolute, 99.8 %), 2–propanol (ACS reagent, 99.8 %), cyclohexane (laboratory reagent, 99.8 %), hydrochloric acid (ACS reagent, 37 %), and sodium hydroxide (ACS reagent, Puriss) were obtained from Honeywell. All the materials were used as received.

2.1.1. Syntheses

Individual syntheses of mesoporous silica (MS) particles with different defined pore diameters are separately described as follows.

2.1.1.1. 2.5–MS. Mesoporous silica particles with 2.5 nm pore diameter were synthesized following the procedure described in detail by Li et al. [30] using surfactant DTAB as a structure–directing agent. According to this procedure, the DTAB was dissolved in water, followed by the addition of 2 M NaOH and heated to the target temperature of 80 °C. In the next step, TEOS was added to the mixture and stirred for another 2 hours. The precipitated dispersion was filtered and washed with ethanol. The solid product was dried at room temperature overnight. The molar ratio of reagents used in the synthesis was TEOS:DTAB:2 MNaOH:H_2O = 1.0:1.8:1.1:1178.0. The material 2.5–MS was gained after the calcination step described below.

2.1.1.2. 3.0–MS. Mesoporous silica particles with 3.0 nm pore diameter, according to N_2 sorption analysis, were synthesized by following the room temperature preparation of MCM–48 material (Mobil Composition of Matter No. 48) presented by Schumacher et al. [31]. CTAB was dissolved in water and ethanol and, after 10 minutes of stirring at 400 rpm, 25 % ammonia hydroxide solution was added. TEOS was added after another 10 minutes of stirring, and the molar ratio of reactants was as follows: TEOS:CTAB:NH_3:EtOH:H_2O = 1.0:0.4:10.8:66.5:170.0. The mixture was stirred during the night at room temperature, and in the next step the material was filtered and washed with ethanol. The sample was dried at room temperature overnight. The material 3.0–MS was prepared after the calcination program described below.

2.1.1.3. 3.5–MS. The material with approximately 3.5 nm pore diameter, according to N_2 sorption, corresponds to the mesoporous material MCM–41 (Mobil Composition of Matter No. 41) and was synthesized following the procedure described by Li et al. [30]. Briefly, CTAB was dissolved in deionized water followed by the addition of NaOH, heated to the target temperature of 80 °C and with the addition of TEOS. After stirring at 80 °C for 2 hours, the dispersion was filtered and washed with ethanol. The molar ratio of the reagent of the described procedure was as follows: TEOS:CTAB:2 MNaOH:H_2O = 1.0:1.8:1.1:1178.0. The product was dried at room temperature during the night. The material was calcined by the temperature program described below.

2.1.1.4. 7.0–MS. The material 7.0–MS corresponds to the mesoporous material SBA–15 (Santa Barbara Amorphous 15) and was synthesized by following the procedure described by Zhao et al. [32]. Briefly,

triblock copolymer, poly(ethylene glycol)–poly(propylene glycol)–poly (ethylene glycol) (pluronic 123) was dissolved in HCl solution and the mixture was stirred for 2 hours at 35 °C. In the next step, TEOS was added drop by drop and the mixture was stirred for 20 hours at 35 °C and then 48 hours at 100 °C. Afterwards, the precipitated dispersion was filtered, washed with deionized water, and dried at room temperature. The filtered product was calcined by the temperature program described below. The sample, used for selective functionalization (methylation), was not calcined.

2.1.1.5. 10–20–MS. The mesoporous material with broader pore size distribution (according to N_2 sorption) with pore diameter of between 10–20 nm was synthesized by the following procedure, presented by Moeler et al. [33,34] with a few modifications. CTAB, H_2O, NH_3 were mixed and stirred for 1 hour at room temperature. The mixture was then heated to 60 °C and stirred at 300 rpm for 1 hour. The mixture of TEOS, iPropanol, and cyclohexane was premixed and added drop by drop. The obtained mixture was stirred for 20 hours at 60 °C. The molar ratio of reagent of the described procedure was as follows: TEOS:CTAB:NH_3:H_2O:CH = 1.0:1.3:0.3:372.1:20.5. The precipitated product was filtered and washed with water. The filtrate was dried in air and then calcined using the program described below.

2.1.1.6. Non-porous silica particles. Non-porous silica particles were synthesized following Stöber procedure described elsewhere. Briefly, TEOS was dissolved in EtOH during the heating to 40 °C, followed with the drop by drop addition of ammonia solution and H_2O, respectively. In the next step the mixture was stirred for 1 h at 40 °C. The precipitated product was filtered, washed with water and dried in air. The molar ratio of reagent in the described procedure was TEOS:EtOH:NH_3:H_2O = 1.0:43.7:1.9:19.6.

2.1.1.7. Calcination and storage of the samples. Dry samples were placed in the oven and the following temperature program was used for calcination in air: heating with a temperature ramp of 1 K/min to 550 °C, maintaining the temperature at 550 °C for 6 hours, and cooling at a rate of 2 K/min. Dried samples were stored in the nitrogen atmosphere until they were used.

2.1.1.8. Selective functionalization (methylation) of external surface of sample 7.0–MS. The synthesized material 7.0–MS (the synthesis is described above) was dried under the vacuum (approximately 10 mbar) and at 100 °C for 2 hours. One gram of the sample was placed in the nitrogen–filled round–bottomed flask and sealed with a rubber stopper. In the next step, 30 ml of dry toluene was added, and the mixture was exposed to an ultrasonic bath for 15 minutes. During the stirring, 0.01 mol of trimethoxymethylsilane was added drop by drop and the mixture was stirred during the night under the reflux. The next day, the sample was filtered and washed with toluene. The filtrate was dried at room temperature conditions during the night. In the next step, the sample was placed in the round–bottomed flask and refluxed during the night in the mixture of HCl and ethanol in order to remove the pluronic 123 from the pores, and filtered and washed with ethanol. Filtrate was firstly dried at room temperature conditions during the night, followed by 2 h drying under the vacuum (approximately 10 mbar) and 100 °C. The sample was stored in a nitrogen atmosphere.

2.1.1.9. Functionalization of non-porous silica particles. As synthesized non-porous samples were dried and functionalized using the same procedure as described above for selective functionalization of external surface, except the last step – reflux during the night after functionalization, was not performed. Samples are in the text marked as methylated non-porous silica particles.

2.1.1.10. Preparation of material with integrated dye. The integration of the MB dye in the mesoporous matrixes was achieved by physical mixing. The materials 3.0–MS, 3.5–MS, 7.0–MS, Me–7.0–MS and methylated non-porous silica particles were mixed with MB dye in the agate pestle and mortar for 15 minutes. The mass ratio of MB:mesoporous silica particles was 1:100; the obtained samples have the following labels: MB–3.0–MS, MB–3.5–MS, MB–7.0–MS, and MB–Me–7.0–MS (see Table 1).

Table 1
Sample labels of mesoporous SiO_2 particles with integrated dye and methylated external surface, used in the scope of this paper.

Sample labels	Average pore diameters and standard deviation (nm)[a]	Integrated dye	Methylated external surface
2.5-MS	2.5±0.4	No	No
3.0-MS	3.0±0.2	No	No
3.5-MS	3.5±0.5	No	No
7.0-MS	7.2±0.7	No	No
10-20-MS	18.2±3.5	No	No
MB-3.0-MS	2.9±0.2	Yes	No
MB-3.5-MS	3.5±0.4	Yes	No
MB-7.0-MS	6.9±0.8	Yes	No
Me-7.0-MS	7.1 ±0.7	No	Yes
MB-Me-7.0-MS	7.1±0.8	Yes	Yes

[a] According to BJH pore size distribution results.

2.2. Methods

The properties of synthesized mesoporous SiO_2 particles (MS particles) were studied in tablet form; each sample was prepared from approximately 70 mg of the powder sample using compression of 500 kg for 1 minute. A disk with a diameter of 0.6 cm was formed.

2.2.1. Morphological and structural properties

The morphological properties of samples were investigated utilizing transmission electron microscopy (TEM) using a Jeol ARM–200 CF microscope operated at 80 kV. Field Emission Scanning Electron Microscopy (FE-SEM, Zeiss ULTRA plus, Germany) operated at accelerating voltage of 1 kV was used was used to investigate non-porous silica particles. The nitrogen sorption isotherm was characterized at 77 K using nitrogen sorption and an ASAP Micromeritics analyzer. Samples (approximately 70 mg) were outgassed at 120 °C for 2 hours. The pore size distribution was analyzed using the BJH (Barrett, Joyner, and Halenda) method.

The structural ordering of the pore channels was characterized using the small–angle x–ray scattering (SAXS) results obtained by an in–lab modified Kratky camera (Anton Paar KG, Graz, Austria) attached to a conventional X–ray generator (GE Inspection Technologies, SEIFERT ISO–DEBYEFLEX 3003) using the primary beam with a wavelength $\lambda = 0.154$ nm (Cu anode operating at 40 kV and 50 mA). The Göbel mirror and the block–collimation system was used to shape a line–collimated monochromatic primary beam. The measurements were recorded for 15 minutes by the Mythen 1 K microstrip solid–state diode–array detector (Dectris, Baden, Switzerland) in the small–angle regime of scattering vector, q, from 0.065 nm^{-1} to 7 nm^{-1}. The scattering vector is defined as $q = 4\pi/\lambda \cdot \sin(\theta/2)$, where θ is the scattering angle. Obtained data were corrected for background scattering. They are still experimentally smeared due to the finite dimensions of the primary beam.

2.2.2. Humidity indicator properties

Evaluation of the humidity indicator behavior was investigated by gravimetrical determination of water vapor isotherms at 25 °C, Fourier–transform infrared spectroscopy (FT–IR), and CIELab color space. In CIELab color space the individual color is specified by three values: L*, a*, and b*. L* corresponds to lightness ranging from 0 to

100, the value of a* represents the green–red component, with green in the negative direction and red in the positive direction, and the b* value represents the blue–yellow component, with blue in the negative direction and yellow in the positive direction. The scaling and limits of a* and b* are most often in the range of ± 100, but these can depend on the implementation. The water isothermal measurements were performed on IGA-100 (Hiden Isochema Inc.) sorption analyser at 25 °C in static conditions from vacuum to 29 mbar of water vapor loading (p/po = 0.915). Prior the measurements, the samples were degassed at 100 °C for 12 h. In order to investigate the humidity indicator behavior in terms of FT–IR spectroscopy and color change, samples were exposed to the environment with different relative humidities (33, 53, 58, 69, 75, 79, 83, and 92 %) achieved by saturated solutions of different salts ($MgCl_2$, $Mg(NO_3)_2$, NaBr, KI, NaCl, NH_4Cl, KCl, mixture of KNO_3, and K_2SO_4), [35,36] respectively, at room temperatures conditions (RT). Before and after the exposure to relative humidity conditions, FT–IR spectra were recorded on exposed samples by a UATR Two Pelkin Elmer spectrophotometer and color variations were evaluated by measurement of CIELab (L*,a*,b*) color space using an i1(X–Rite) colorimeter. The total change of color, indicated by the parameter ΔE^*, was calculated from CIELab measurement results using the following equation:

$$\Delta E^* = \sqrt{(\Delta a^{*2} + \Delta b^{*2} + \Delta L^{*2})} \quad (1)$$

The measurement of color coordinates was performed at three different areas. An average result ΔE^* was presented with the corresponding standard deviation.

3. Results and Discussion

3.1. Morphological, structural and water-sorptive properties of mesoporous silica particles

Morphological, structural, and water-adsorptive properties have been analyzed using nitrogen sorption, SAXS data, TEM microscopy, and water-vapor adsorber. The pore-size distributions of the samples without integrated dye are presented in Fig. 1a which shows that for the particles with various average pore diameters in the range of 2.5 nm to 20 nm, the 2.5, 3.0, 3.5, 7.0, and 10–20 nm pore-diameter materials have been successfully synthesized. As already described in the experimental section, the samples are labelled according to average diameter of the pores, and determined using nitrogen sorption and the BJH method (2.5–MS, 3.0–MS, 3.5–MS, 7.0–MS, and 10–20–MS) as shown in Table 1. The 3.5–MS and 7.0-MS samples exhibit a well-defined hexagonal H2 ordering of pore channels (orange and azure scattering curves are presented in Fig. 1b). Their parallel orientation can be clearly seen in the TEM micrographs in Fig. 2a. In contrast, the pore channels are radially oriented in the case of 2.5–MS, 3.0–MS, and 10–20-MS samples, as depicted in Fig. 2a. Samples 2.5–MS, 3.0–MS, 3.5–MS and 10–20 MS are spherical in shape, whereas 7.0–MS is rod-like. No characteristic well-defined spatial ordering of the pore channels can be identified from the corresponding SAXS curves (red, blue, and magenta curves in Fig. 1b).

Water vapor isotherms (see Fig. 2b) could be classified as an isotherm of type V according to IUPAC directions [1] which are usually observed for water vapor adsorption on mesoporous materials. At the low relative values there is a small amount of water molecules adsorbed mainly through H-bonding to surface –SiOH groups [37] and through molecular clustering [1],while at higher relative humidity the adsorption of water is followed by the capillary condensation of water in the pores and the corresponding filling of the pores with water [1]. The relative humidity ranges leading to the capillary condensation and eventual complete filling of the pores are similar but different for the studied samples with different pore diameter values (see Fig. 2b) as already recognized in the literature [38]. This highlights that in the mesoporous silicas with comparable hydrophilicities the range of the capillary condensation occurrence mainly depends on the pore diameter. As seen in Fig. 2.b, the capillary condensation is achieved at 45 % relative humidity in the sample 2.5–MS; at 55 % relative humidity in the sample 3.0–MS; at 75 % relative humidity in the sample 3.5–MS; while at 85 % relative humidity in the samples 7.0–MS and 10–20–MS.

After integration of the MB dye into the samples with narrow pore size distribution (samples MB–3.0–MS, MB–3.5–MS, and MB–7.0–MS) a slight decrease in the amount of adsorbed nitrogen and also a corresponding slighter decrease in the pore volume of samples with integrated dye was observed for all three samples, as depicted in Fig. 3 (comparison of the black and colored curves). The decrease of the available surface area for nitrogen adsorption after the dye incorporation and the reduction of the volume of the pores indicate that the MB dye was successfully integrated into the pores of samples. Because physical mixing was used for dye incorporation, the dye is also present in the external surface.

3.2. The impact of pore diameters on humidity–indicating behavior

The humidity–indicating function of the samples with the integrated MB dye was evaluated by FT–IR spectroscopy and gravimetrical water vapor sorption analysis in order to gain information about the type of bonded water and its amount, respectively. Color change between solid MB crystals and dissolved MB dye was caused by dissolution in water. Simultaneously, the total color change was sensed by the CIELab color system in order to evaluate the dissolving mechanism of the MB dye in the mesoporous material after the samples were exposed to the

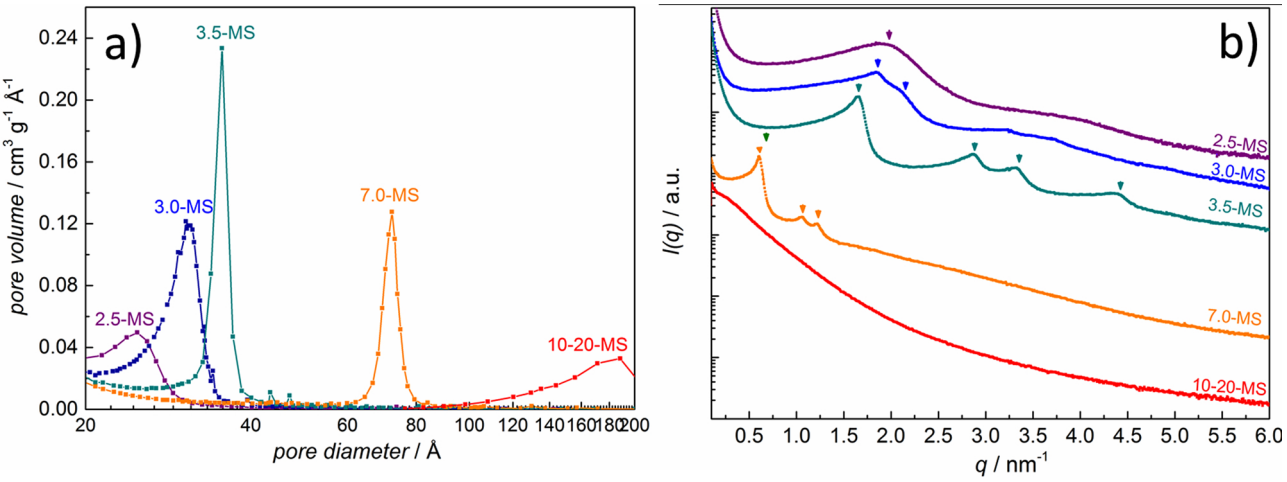

Fig. 1. a) The pore size distribution and b) the SAXS curves of mesoporous silica particles with various pore diameters: 2.5–MS, 3.0–MS, 3.5–MS, 7–MS, 10–20–MS.

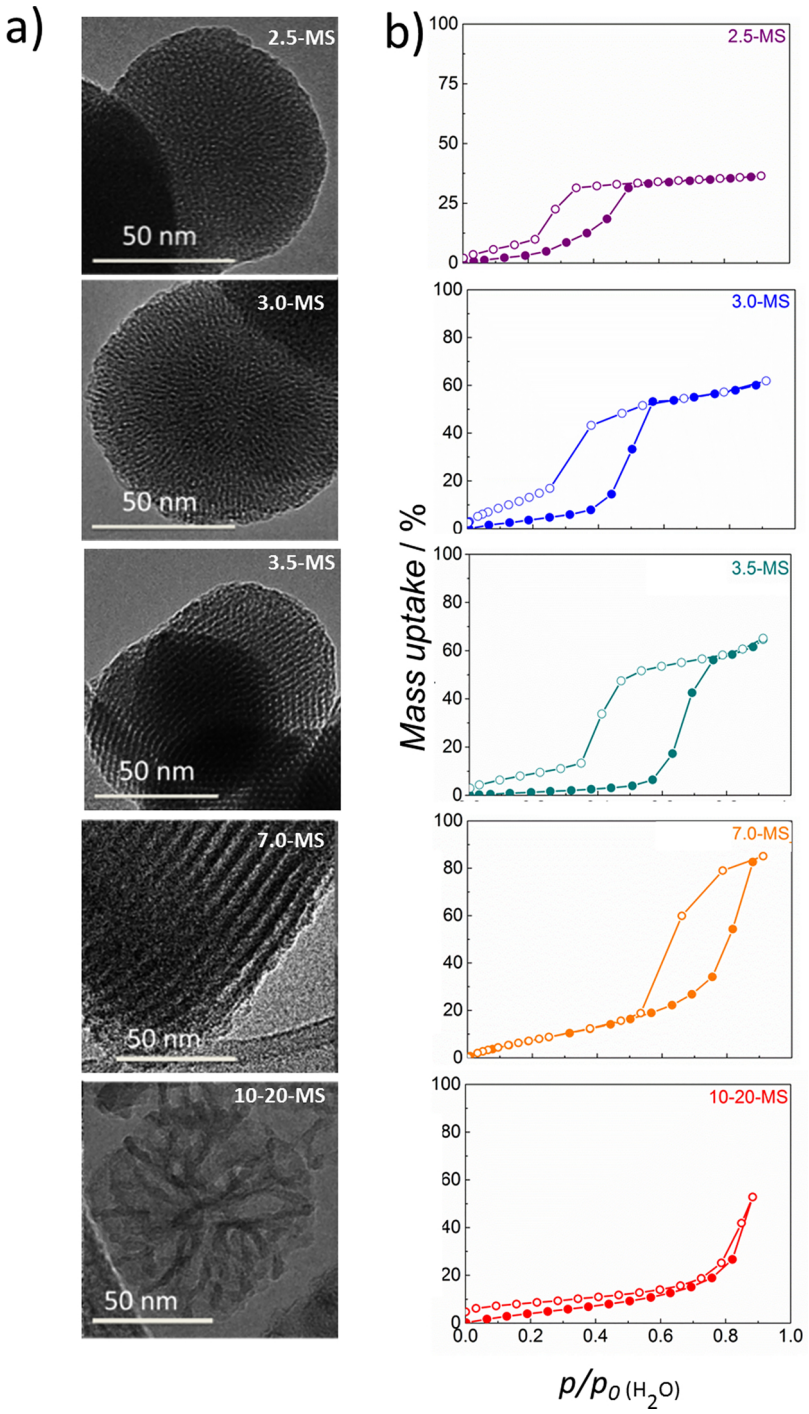

Fig. 2. a) TEM micrographs and b) water vapor sorption isotherms for samples with different defined pore diameters.

environment of different relative humidities. The resulting FT–IR spectra for the samples with integrated dye after the 24–hour exposure are presented in Figs. 4a, 5 a, and 6 a. One can clearly resolve the O–H stretching and O–H bending vibrations in the ranges between 3300–3500 cm^{-1} and 1600–1700 cm^{-1}, respectively, indicating the presence of hydrogen bonds due to the water sorption and condensation in the pores [39]. The MB–3.0–MS sample shows the trend of intensive O–H stretching as also O–H bending vibrations only when the material was exposed to an environment with relative humidity of 53% or higher, as depicted in Fig. 4a. The water vapor isotherm is shown in Fig. 4b and enables a qualitative analysis of the adsorbed concentration of water. It is in good agreement with the results obtained from the FT–IR spectra, as follows. Small concentrations of adsorbed water at low relative humidity (up to 10 %) could be clearly observed. In the relative humidity range of between 40 and 55 % an exponential dependence of the adsorption of water on relative humidity was observed. This range corresponds with the pore filling with liquid water. The additional increase of the relative humidity had negligible influence on the concentration of adsorbed water vapor of the sample (see Fig. 4b). At a relative humidity of 55 % the sample MB–3.0–MS reaches nearly complete capillary condensation. Simultaneous evaluation of the total change of color with 24–hour exposition to the individual relative humidity environment is presented in Fig. 4c. It can be clearly seen that the response in total color change is found to be linear in the relative

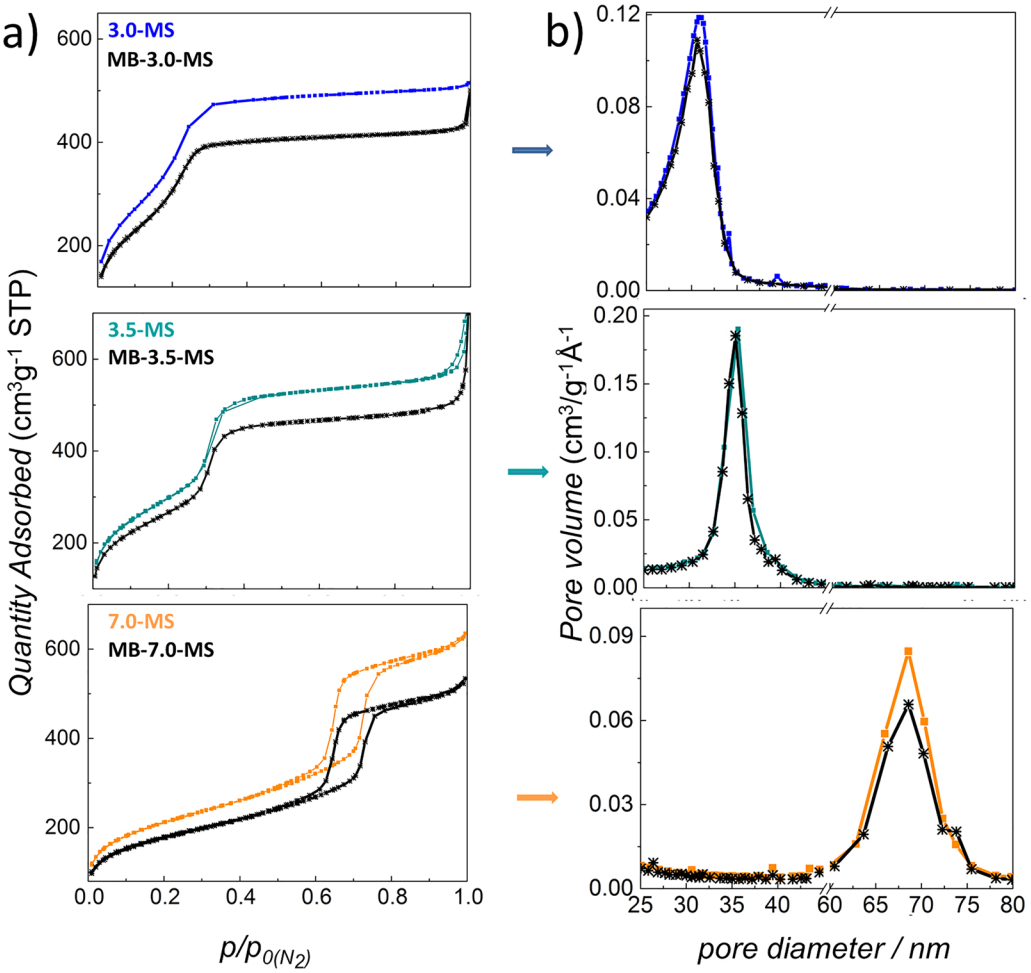

Fig. 3. a) The nitrogen–sorption isotherms and b) the corresponding pore–sized distribution according to the BJH method of samples without the integrated MB dye: 3.0–MS, 3.5–MS, and 7.0–MS (colored curves); and samples with integrated MB dye: MB–3.0–MS, MB–3.5–MS, and MB–7.0–MS (black curves).

humidity range between 53 and 92 % (see Fig. 4**c** and the fitted curves depicted in Fig. S1). One would expect that the color changes after the completed capillary condensation should be in accordance with the changes in the concentration of the adsorbed water (see Fig. 4b and c). The trend discrepancies between isothermal and colorimetric experiments may be the consequence of the dye being adsorbed on the outer surface of the silica materials rather than within the mesopores due to the size limitations. In such cases, the rate of color change (dye dissolving) is not expected to be a function of the water capillary condensation of water within the pores.

The material MB–3.5–MS exhibits the trend of increasing intensity of FT–IR peaks due to O–H stretching and O–H bending vibrations as the material was exposed to relative humidity below 69 % (see red, dark red, and orange curves in Fig. 5a). An additional increase in relative humidity of the environment did not significantly increase the intensity of O–H stretching and O–H bending. The water vapor isotherm also shows pore filling in the relative humidity range between 53 and 79 % and almost complete capillary condensation for the samples exposed to an environment of 79 % and higher, as seen in Fig. 5b. The evaluation of the change in color shows a response already after exposure to the lowest relative humidity values (33 and 53 %), although only up to 10 wt.% of water was adsorbed (see Fig. 5b). One could clearly observe that the filling of pores with water (exposure to relative humidity range between 53 and 79 %) causes the coloring of the sample (see Fig. 5c). In contrast, the exposure of the samples to an even higher relative humidity environment (from 75 to 92 %) did not influence the color drastically (see Fig. 5c and the fitted curves depicted in Fig. S2). One could conclude that the color change in the range of pore filling is exponential and the values reached plateau with capillary condensation of water. It could be clearly observed that the dissolution of the dye could be clearly observed after a smaller amount of adsorbed water.

The increasing trend of the intensity of O–H stretching and O–H bending vibration peaks was also observed for the MB–7.0–MS sample after exposure to environments with different relative humidities and was the most pronounced until relative humidity values of 79 %. The exposure of samples to relative humidity in the range from 85 to 92 % did not influence the intensities of FT–IR peaks significantly, as shown in Fig. 6a. According to the water absorption isotherm, pore filling is exhibited in the range between 75 and 85 %, and completed with capillary condensation achieved at 88 %, as shown in Fig. 6b. The evaluation of the color change shows linear response in almost the whole range of relative humidity (the values between 58 and 79 % could be fitted linearly; see lines in Fig. S3), which also suggests the dye dissolution occurrence even before the start of water condensation in pores.

Although the tested mesoporous materials exhibit different sorption isotherms of water in respect to the pore size distribution, as clearly seen in Figs. 3b, 4 b, 5 b, and 6 b, the total color change does not follow the trend in the adsorbed water concentration in all cases, as revealed in Figs. 4c and 6 c. Therefore, the desired outcome of our study, in the sense that the capillary condensation could be recognized as the key trigger for dissolution of the integrated dye in the pores, was unfortunately not clearly observed. Specifically, although the materials MB–3.0–MS and MB–7.0–MS exhibit the initiation of capillary

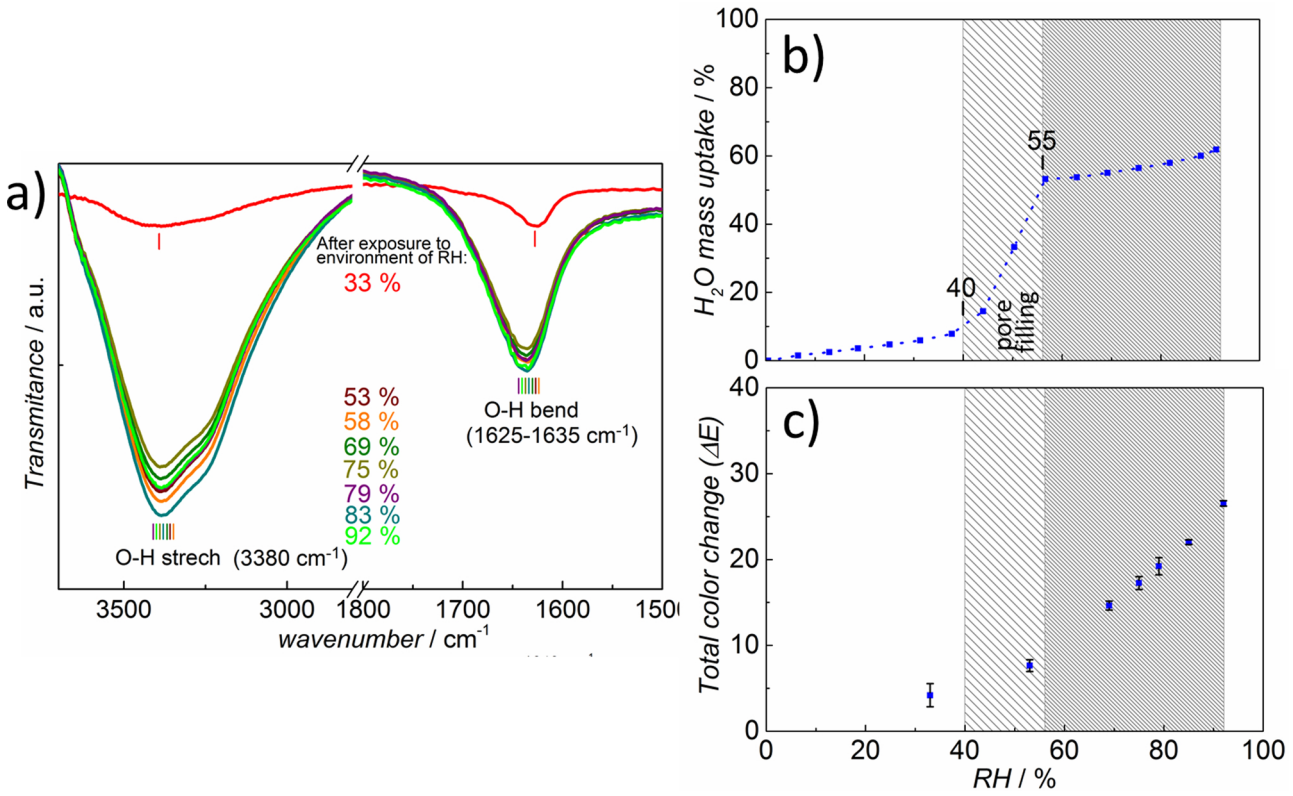

Fig. 4. a) FT–IR spectra, b) water vapor isotherm, and c) total color change of sample MB–3.0–MS after exposure to different relative humidity environments.

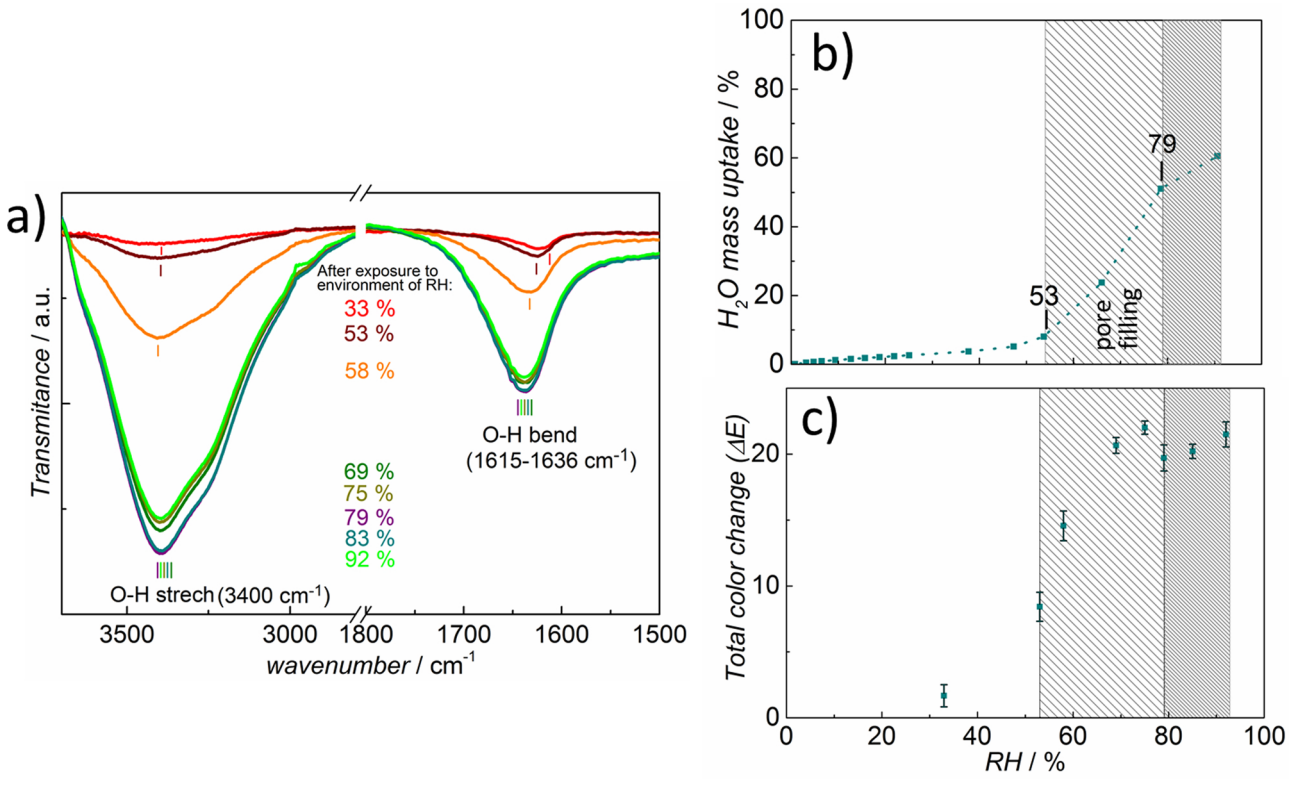

Fig. 5. a) FT–IR spectra, b) water vapor isotherm, and c) total color change for sample MB–3.5 after exposure to environment of different relative humidities.

condensation at much different relative humidity values (see Figs. 4b and 6 b) the detected color changes (indicating the dissolution of the dye in the pores) exhibit very similar courses in both cases. This outlines that already appear in the initial stages of water adsorption on the surface of the pore walls influence the color change significantly, as also seen in Figs. 4c, 5 c, and 6 c. These results indicate that to gain the desired response of the studied mesoporous materials with various pore diameters in terms of relative humidity indicator behavior, one should

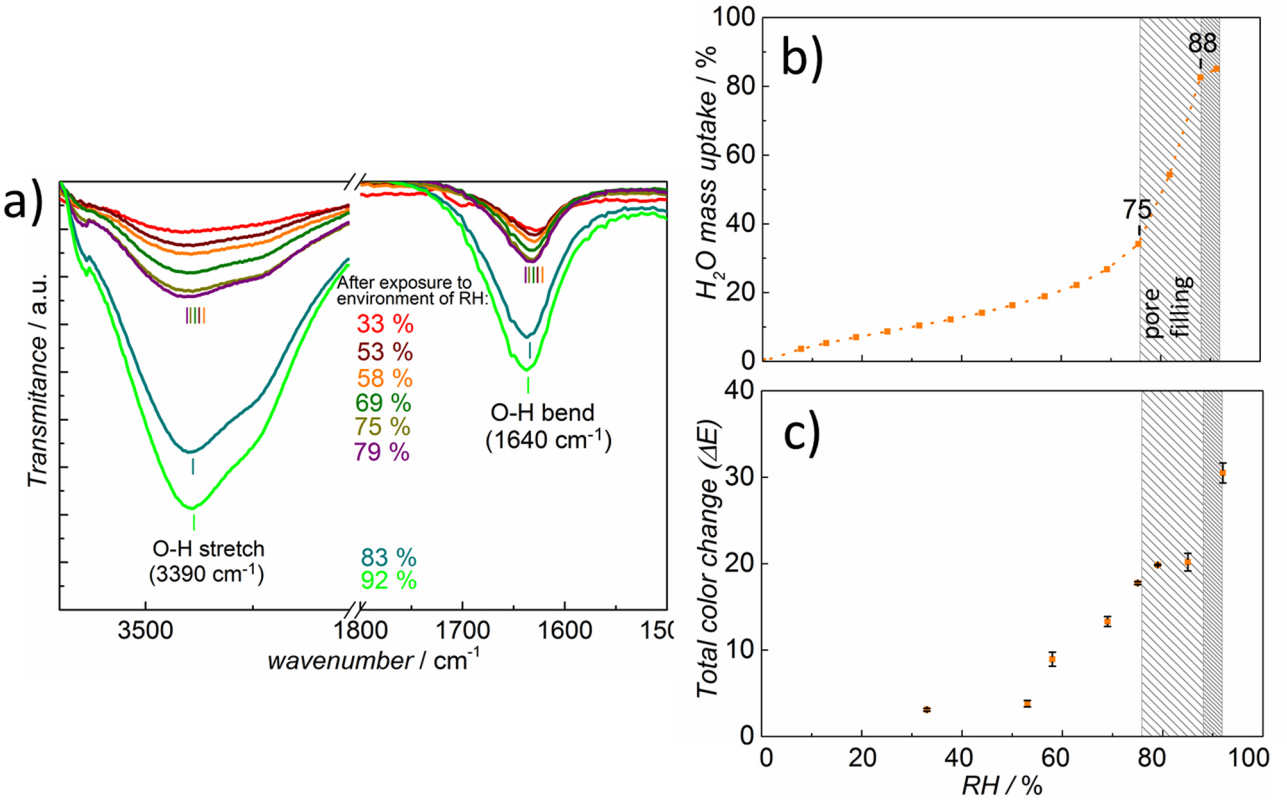

Fig. 6. FT–IR spectra, b) water vapor isotherm, and c) total color change for sample MB–7.0 after exposure to different water vapors.

achieve a cutoff response at some specific value of relative humidity. This means that the dye dissolution at low relative humidity values, prior to the occurrence of the capillary condensed water, should be somehow inhibited and minimized. In order to decrease the effect of water adsorption to the external surface of mesoporous particles, we hydrophobized the external surface of these particles; the selective functionalization (methylation) of the external surface was tested on the mesoporous material sample 7.0–MS.. The bands at 1297 cm^{-1} and at 1379 cm^{-1} in FT-IR spectrum belong to Si-CH_3 and C-H vibrations, respectively, of functionalized sample (Me-7.0-MS, see Supplementary data – Figure S4), which confirms the presence of umbrella mode in methylsilanes and therefore methylation of the sample.

3.3. The impact of selective external functionalization on humidity indicating function

The resulting FT–IR spectra of the mesoporous material 7.0–MS with the methylated external surface of the mesoporous particles and with the pore–integrated dye (MB–Me–7.0–MS) after their exposure to environments of different relative humidities, are presented in Fig. 7a. The increasing trend of the intensity of O–H stretching and O–H bending vibration peaks can be clearly observed, especially in the case of the samples exposed to the highest relative humidity values. According to this isotherm, the concentration of the adsorbed water is still less than 10 % at the relative humidity of 80 %. However, with exposure to relative humidity higher than 85% (see Fig. 7b), the concentration of adsorbed water increases exponentially. The evaluation of the color change with such an exposure, depicted in Fig. 7c, shows negligible color change for the environments with relative humidity below or equal to 80 %. Increasing the relative humidity from 80 % up to 92 % causes a considerable change in the color of the sample ($\Delta E^* = 25$), which can be considered as the well–defined cutoff response in this range of relative humidity. Inspecting the curves in Fig. 7b and c, one can conclude that the pronounced response occurs in the range of the relative humidity corresponding to the capillary condensation regime.

Because pluronic 123 was removed after surface functionalization was performed, it can be assumed that mainly the external surface was methylated. The selectively methylated mesoporous surface of MB–Me–7.0–MS is reflected in the decrease in the concentration of adsorbed water in lower relative humidity environments, in the capillary condensation of water at higher relative humidity (see Fig. 7b), and in the color change occurring at the highest relative humidity values (see Fig. 7c). To investigate the influence of mesopores in SiO_2 particles (Fig. S5), the surface of non-porous silica particles (BJH pore size distribution is presented in Fig. S5-a and FE-SEM micrograph in Fig. S5-b) were methylated and mixed with methylene blue dye (BJH pore size distribution presented in Fig. S5-c). After exposure to different RH conditions it could be clearly observed the color change in the whole range of RH is minor, invisible to the naked eye (see Fig. S5-d), which confirms the effect of pore filling is crucial to obtain the cutoff color response to RH in methylated samples.

The proposed mechanism of water adsorption to the non–selective functionalized 7.0–MS and selective functionalized Me–7.0–MS is schematically presented in Fig. 8. We assumed that the water–sorption on the non–functionalized surface of MB–7.0–MS samples (see Fig. 8–left) occurs by H–bonding with the Si–OH groups on the mesoporous particle external surface and by H–bonding with the Si–OH groups on the internal surface of the pores, and by the capillary condensation that followed the adsorption step. The dissolving of the dye was therefore observed through the whole range of relative humidity (see photo in Fig. 8a), whereas the water–sorption on the selectively functionalized surface of the samples MB–Me–7.0–MS (Fig. 8b) occurs mainly by the H–bonding with Si–OH groups in the pores and by the capillary condensation that followed the adsorption step. Due to the hydrophobic –CH_3 groups on the surface (see Fig. 8b), the dissolving of the dye is observed only in the range of very high relative humidity which caused capillary condensation in hydrophilic pores regardless of

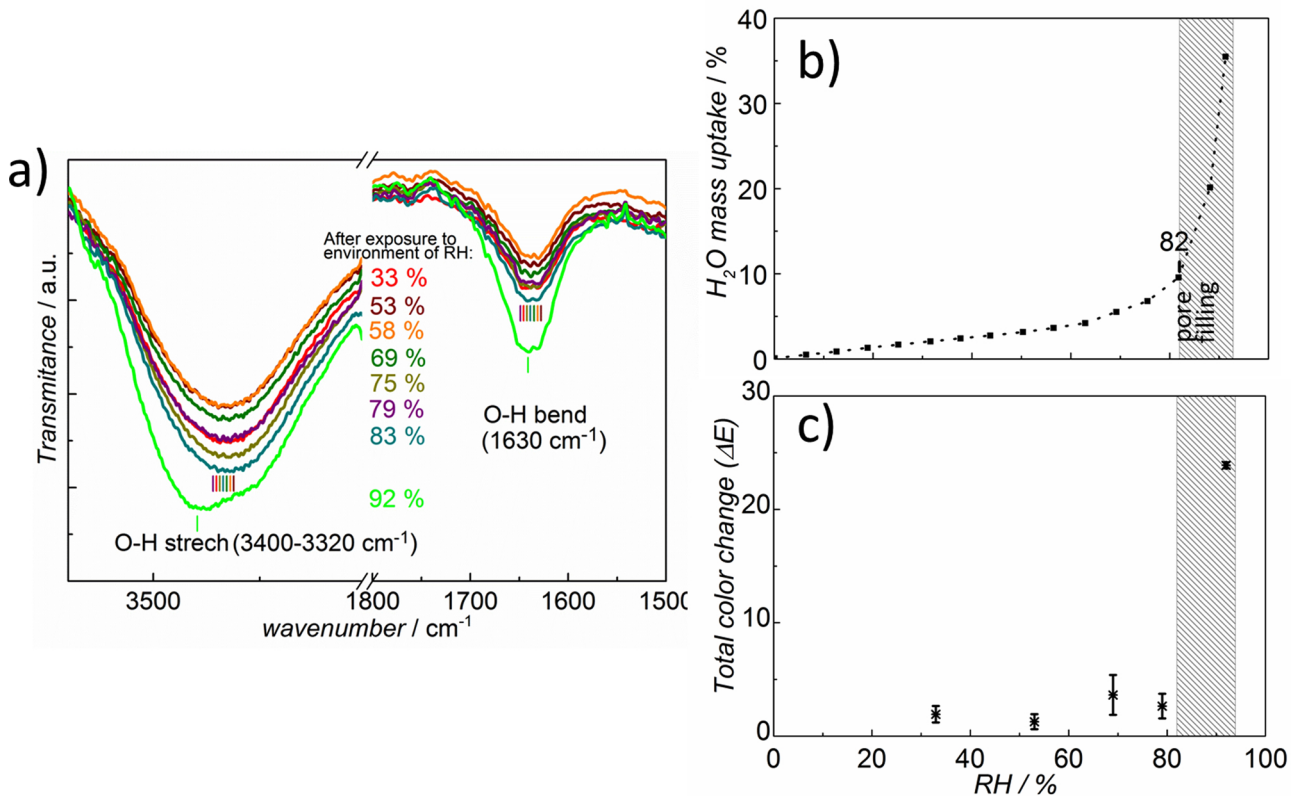

Fig. 7. a) FT–IR spectra, b) water vapor isotherm, and c) total color change for sample Me–MB–7.0– after exposure to environment of different water vapor pressures.

the hydrophobic mesoporous particle's external surface (see Fig. 8b photo) and showed the corresponding cutoff response. In contrast, we assumed the methylation of non-porous silica surface (Fig. S5) distribute the $–CH_3$ groups through the whole surface (Fig. S6) and therefore prevents the water adsorption and therefore corresponding dissolution of the dye.

4. Conclusion

We investigated a novel advanced concept of colorimetric indication of narrow range of relative humidity based on capillary condensation of water in SiO_2 mesopores. To this end, we have synthesized mesoporous silica materials with the defined uniform pore diameters of 3.0, 3.5, and 7.0 nm and integrated methylene blue dye into their pores. The incorporation of dye into the pores was proved by the reduced volume of pores from nitrogen sorption analysis. The relative humidity indicating

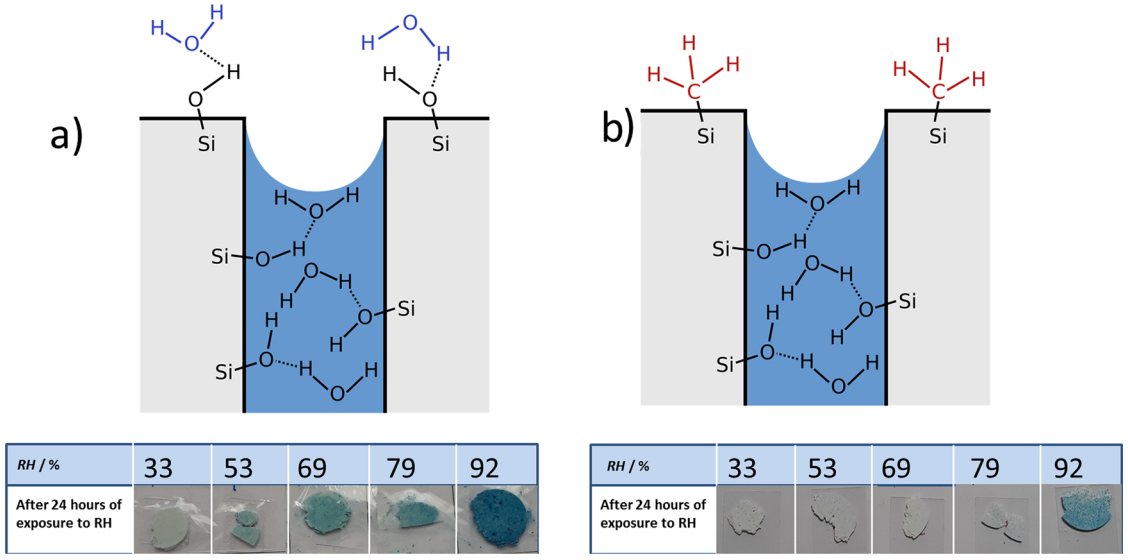

Fig. 8. The schematic representation of the pore channel of the mesoporous material after 24–hour exposure to an environment with 92 % relative humidity: (a) with non–methylated (MB–7.0–MS) and (b) methylated external surface (MB–Me–7.0–MS). Bottom: photos of the samples (a) MB–7.0–MS and (b) MB–Me–7.0–MS exposed to environments of different relative humidities as indicated by the given values.

function was tested utilizing the gravimetrical analysis of the adsorbed water vapor and FT–IR spectroscopy—different sorption isotherms of water were observed for materials with different pore diameters. We proved that the diameter of mesopores with comparable hydrophobicity is in strong relation with the value of relative humidity when complete capillary condensation occurred. The samples with pores of diameter of 3.0 nm, 3.5 nm, and 7.0 nm reached complete capillary condensation when exposed to an environment with 55, 79, and 88 % relative humidity, respectively. We found out that the methylene blue adsorbed on the surface of mesoporous SiO_2 can be dissolved with increasing RH, resulting in significant blue coloration and increase of total color change determined in CIELab color space. However, the color change occurred already at lower relative humidity values, prior to the capillary condensation range. By this reason these materials did not show proper humidity–indicating function and could not be properly used in this sense. In order to achieve the dissolution of the dye in the narrow range of relative humidity, the external surface of the selected mesoporous particles was selectively methylated. The modification of the surface of the particles was confirmed by achieving the decreased concentration of adsorbed water at lower relative pressures of water vapor and the coexistence of the capillary condensation at higher relative pressures. In this material, the change of color was restricted to a narrow range of relative humidity, coinciding with the range of capillary condensation. The presence of mesopores was crucial for functioning system, as methylated non-porous silica particles did not yield the color change of their porous counterparts. The presented results demonstrate that we reached our objective and that a relative–humidity–indicating cutoff function based on capillary condensation in the mesopores is indeed possible and can be gained only after modification of the particles' external surface. The verified concept forms a basis for future optimization of the colorimetric humidity–indicating porous systems, including the study of pore diameter of methylated materials on colorimetric response and its reversibility.

Author Contributions

The manuscript was written through contributions of all authors. All authors have given approval to the final version of the manuscript.

CRediT authorship contribution statement

Erika Švara Fabjan: Conceptualization, Investigation, Writing - original draft, Writing - review & editing. **Peter Nadrah:** Investigation, Writing - review & editing. **Anja Ajdovec:** Investigation. **Matija Tomšič:** Investigation, Writing - review & editing. **Goran Dražić:** Investigation. **Matjaž Mazaj:** Investigation, Writing - review & editing. **Nataša Zabukovec Logar:** Writing - review & editing. **Andrijana Sever Škapin:** Writing - review & editing.

Declaration of Competing Interest

The authors declare that they have no known competing financial interests or personal relationships that could have appeared to influence the work reported in this paper.

Acknowledgements

We acknowledge the financial support from the Slovenian Research Agency through post–doctoral project No. Z1–8149 and the core research funds No. P2–0273, No. P1–0201, No. P1-0021, and No. P2–0393. Matija Tomšič is most grateful to Prof. Otto Glatter for his generous contribution to the instrumentation of the Light Scattering Methods Laboratory in Ljubljana. We are also very grateful to Dr. Oleksii Pliekhov for his help in water sorption measurement.

Appendix A. Supplementary data

Supplementary material related to this article can be found, in the online version, at doi:https://doi.org/10.1016/j.snb.2020.128138.

References

[1] M. Thommes, K. Kaneko, A.V. Neimark, J.P. Olivier, F. Rodriguez–Reinoso, J. Rouquerol, K.S.W. Sing, Pure Appl. Chem. 87 (2015) 105, https://doi.org/10.1515/pac-2014-1117.
[2] B.J. Melde, B.J. Johnson, P.T. Charles, Sensors 8 (2008) 5202, https://doi.org/10.3390/s8085202.
[3] T.A. Blank, L.P. Eksperiandova, K.N. Belikov, Sens. Actuators, B 228 (2016) 416, https://doi.org/10.1016/j.snb.2016.01.015.
[4] S.H. Wu, C.Y. Mou, H.P. Lin, Chem. Soc. Rev. 42 (2013) 3862, https://doi.org/10.1039/C3CS35405A.
[5] V.K. Tomer, S. Devi, R. Malik, S.P. Nehra, S. Duhan, Microporous Mesoporous Mater. 219 (2016) 240, https://doi.org/10.3390/ma10050535.
[6] J.C. Tu, N. Li, W.C. Geng, R. Wang, X.Y. Lai, Y. Cao, T. Zhang, X.T. Li, S.L. Qiu, Sens. Actuators, B 166 (2012) 658, https://doi.org/10.1016/j.snb.2012.03.033.
[7] V.K. Tomer, S. Duhan, Sens. Actuators, B 220 (2015) 192, https://doi.org/10.1016/j.snb.2015.05.072.
[8] V.K. Tomer, S. Duhan, R. Malik, S.P. Nehra, S. Devi, J. Am. Ceram. Soc. 98 (2015) 3719, https://doi.org/10.1111/jace.13836.
[9] M. Anbia, M. Neyzehdar, A. Ghaffarinejad, Sens. Actuators, B 193 (2014) 225, https://doi.org/10.1016/j.snb.2013.11.068.
[10] R.R. Qi, X.Z. Lin, J.X. Dai, H.R. Zhao, S. Liu, T. Fei, T. Zhang, Sens. Actuators, B 277 (2018) 584, https://doi.org/10.1016/j.snb.2018.09.062.
[11] H.R. Zhao, T. Zhang, J.X. Dai, K. Jiang, T. Fei, Sens. Actuators, B 240 (2017) 681, https://doi.org/10.1016/j.snb.2016.09.030.
[12] IEA, Annex 14: Condensation and Energy, Vol. 2: Guide-lines and Practice, International Energy Agency, 1990.
[13] I.B. Burgess, M. Loncar, J. Aizenberg, J. Mater. Chem. C 1 (2013) 6075, https://doi.org/10.1039/C3TC30919C.
[14] A.P. Russell, K.S. Fletcher, Anal. Chim. Acta 170 (1985) 209, https://doi.org/10.1016/S0003-2670(00)81744-4.
[15] A. Kharaz, B.E. Jones, Sens. Actuators, A 47 (1995) 491, https://doi.org/10.1016/0924-4247(94)00948-H.
[16] A. Tsigara, G. Mountrichas, K. Gatsouli, A. Nichelatti, S. Pispas, N. Madamopoulos, N.A. Vainos, H.L. Du, F. Roubani-Kalantzopoulou, Sens. Actuators, B (2007) 120481, https://doi.org/10.1016/j.snb.2006.02.046.
[17] M. Bedoya, M.T. Diez, M.C. Moreno-Bondi, G. Orellana, Sens. Actuators, B 113 (2006) 573, https://doi.org/10.1016/j.snb.2005.07.006.
[18] S. Otsuki, K. Adachi, T. Taguchi, Sens. Actuators, B 53 (1998) 91, https://doi.org/10.1016/S0925-4005(98)00296-2.
[19] T.E. Brook, M.N. Taib, R. Narayanaswamy, Sens. Actuators, B 38-39 (1997) 272, https://doi.org/10.1016/S0925-4005(97)80217-1.
[20] I.M. Raimundo Jr., R. Narayanaswamy, Analyst 124 (1999) 1623, https://doi.org/10.1039/A905264J.
[21] H. Dacres, R. Narayanaswamy, Talanta 69 (2006) 631, https://doi.org/10.1016/j.talanta.2005.10.037.
[22] M.A. Zanjanchi, Sh. Sohrabnezhad, Sens. Actuators, B 105 (2005) 502, https://doi.org/10.1016/j.snb.2004.07.009.
[23] E. Horvath, P. Rebernik Ribič, F. Hashemi, L. Forro, A. Magrez, J. Mater. Chem. 22 (2012) 8778, https://doi.org/10.1039/C2JM16443D.
[24] M.D. Fernández-Ramos, Y.F. Ordónez, L.F. Capitán-Vallvey, I.M. Pérez de Vargas-Sansalvador, J. Ballesta-Claver 220 (2015) 528, https://doi.org/10.1016/j.snb.2015.06.006.
[25] S.A. Kolpakov, N.T. Gordon, C.B. Mou, K.M. Zhou, Sensors 14 (2014) 3986, https://doi.org/10.3390/s140303986.
[26] J.M. Corres, I.R. Matias, M. Hernaez, J. Bravo, F.J. Arregui, IEEE Sensors Journal 8 (2008) 281, https://doi.org/10.1109/JSEN.2008.917487.
[27] Z.J. Zhao, Y.X. Duan, Sens. Actuators, B 160 (2011) 1340, https://doi.org/10.1016/j.snb.2011.09.072.
[28] J. Estella, P. de Vicente, J.C. Echeverria, J.J. Garrido, Sens. Actuators, B 149 (2010) 122, https://doi.org/10.1016/j.snb.2010.06.012.
[29] P.R. Ginimuge, S.D. Jyothi, J Anaesthesiol Clin Pharmacol. 26 (4) (2010) 517.
[30] Z.X. Li, J.L. Nyalosaso, A.A. Hwang, D.P. Ferris, S. Yang, G. Derrien, C. Charnay, J.O. Durand, J.I. Zink, J. Phys. Chem. C 115 (2011) 19496, https://doi.org/10.1021/jp2047147.
[31] K. Schumacher, M. Grun, K.K. Unger, Microporous Mesoporous Mater. 27 (1999) 201, https://doi.org/10.1016/S1387-1811(98)00254-6.
[32] D.Y. Zhao, J.L. Feng, Q.S. Huo, N. Melosh, G.H. Fredrickson, B.F. Chmelka, G.D. Stucky, Science 279 (1998) 548, https://doi.org/10.1126/science.279.5350.548.
[33] K. Moller, T. Bein, Chem. Mater. 29 (2017) 371, https://doi.org/10.1021/acs.chemmater.6b03629.
[34] K. Moller, J. Kobler, T. Bein, Adv. Funct. Mater. 17 (2007) 605, https://doi.org/10.1002/adfm.200600578.
[35] L. Greenspan, J. Res. Natl. Bur. Stand., Sect. A 81 (1977) 89, https://doi.org/10.6028/jres.081a.011.
[36] D. Kitic, M.L. Pollio, G.J. Favetto, J. Chirife, J. Food Sci. 53 (1988) 578, https://doi.org/10.1111/j.1365-2621.1988.tb07761.x.
[37] B. Grunberg, T. Emmler, E. Gedat, I. Shenderovich, G.H. Findenegg, H.H. Limbach,

G.B. Buntkowsky, Chem. - Eur. J. 10 (2004) 5689, https://doi.org/10.1002/chem.200400351.
[38] J. Hwang, S. Kataoka, A. Endo, H. Daiguji, J. Phys. Chem. C 119 (2015) 26171, https://doi.org/10.1021/acs.jpcc.5b08564.
[39] E.P. Ng, S. Mintova, Microporous Mesoporous Mater. 114 (2008) 1, https://doi.org/10.1016/j.micromeso.2007.12.022.

Erika Švara Fabjan is a researcher at the Department of materials at Slovenian National Building and Civil Engineering Institute. She received her Ph.D. degree in Chemical sciences in 2015 at Faculty of chemistry and chemical technology, University of Ljubljana. Her research interests include synthesis and characterization of various functional materials, especially based on various porous structures with defined and non-defined porosity.

Peter Nadrah is a researcher at the Slovenian National Building and Civil Engineering Institute. His research interests include functional mesoporous silica materials and photocatalytic materials.

Matija Tomšič is an associate professor in Physical Chemistry at the Chair of Physical Chemistry, Faculty of Chemistry and Chemical Technology, University of Ljubljana, Slovenia. His main research interests are the structure, dynamics and structure-function relationships in various chemical, colloidal and hierarchically organized systems that are interesting for different nanotechnological applications. In his research, he is combining different experimental and theoretical approaches connected to the scattering methods, mainly small- and wide-angle x-ray scattering (SWAXS) and the static and dynamic light scattering (SLS, DLS).

Nataša Zabukovec Logar is a Head of the Department of Inorganic Chemistry and Technology at the National Institute of Chemistry in Ljubljana and Full Professor of Chemistry at the University of Nova Gorica. She has more than 25 years of experience in the research in the field of porous materials for energy and environmental applications. Her research emphases are development of new materials for heat storage and CO2 capture/conversion, as well as studies of porous solids for their use in wastewater and drinking water treatment.

Andrijana Sever Škapin is an experienced scientist in the field of materials science. Besides published several papers in highly ranked international journals she is also the co-author of four patents in the scope of new materials and processes for monitoring of harmful UV lights, consolidation of valuable materials and cleaning of water, respectively. All inventions indirectly influences on peoples' health and quality of life, so these inventions imply exceptional socio-economic achievements. She has leaded or had the main role in several applied national and international research projects where the key role was development of new functional materials.